Proceedings of ASME TURBO EXPO 2006
Power for Land, Sea, and Air
May 8-11, 2006, Barcelona, Spain

GT2006-91011

Influence of Casing Roughness on the Aerodynamic Structure of Tip Vortices in an Axial Flow Turbine

Nikhil M. Rao[1], Baris Gumusel[2], Levent Kavurmacioglu[3], Cengiz Camci[4]

Turbomachinery Aero-Heat Transfer Laboratory
Department of Aerospace Engineering
The Pennsylvania State University

223 Hammond Building, University Park, PA 16802

ABSTRACT

The aerodynamic influence of casing surface roughness on over-tip-leakage flow was investigated in a large scale, rotating, axial turbine rig. Phase-locked measurements of the absolute total pressure in a cold flow turbine research facility were conducted at the turbine stage exit using a high-frequency-response total pressure probe. Time accurate measurements provided valuable aerodynamic information quantifying the near tip flow modifications imposed by artificially roughened casing inner surface. A partial segment of the turbine casing was roughened by using a roughness layer of two different mean roughness heights. A smooth wall as a baseline case was also investigated by attaching a smooth layer of equivalent thickness to the casing surface. Artificially roughening the casing surface significantly reduced the leakage mass flow rate and the momentum deficit in the core of the tip vortex. The reductions obtained in the tip vortex size and strength influenced the tip-side passage vortex and other typical core flow characteristics in the passage. The influence of casing roughness was studied in a range of tip clearance values.

INTRODUCTION

The current study aims to improve our physical understanding of axial turbine tip leakage flow under the influence of artificially imposed casing roughness. Although there have been many recent studies in understanding the influence of roughness on aerodynamic efficiency or losses in turbomachinery systems, our knowledge on the influence of artificially introduced wall roughness applied on the inner part of the casing is very limited. Experiments with artificially roughened casing around the rotor tip area are performed in the Axial Flow Turbine Research Facility AFTRF at the Pennsylvania State University. The main goal of the study is to investigate if the artificial roughening of the casing surface facing the rotor blade tips could be used to reduce the tip leakage mass flow rate in an effort to improve turbine stage performance.

The present study also addresses the influence of the relative motion of the outer casing using a computational study. The details of the aerodynamic structure in the rotor passages are visualized with a relative casing velocity which is the same as the actual tip speed of the rotor. The relative flow in the rotor passage is also computationally predicted using a stationary casing which resembles the AFTRF relative rotor flow in a cascade environment where there is no casing motion is imposed.

The influence of surface roughness character on the flow near a rough wall has been studied by many researchers in the past. First fundamental studies in this area were conducted by Nikuradse [1] and Schlichting [2]. Most of the past studies use an equivalent sandgrain roughness size k_s representing a measure of the size of sand grains used on the surface. Relative to smooth surfaces, they found significant augmentations of mixing and turbulent transport in the boundary layers developing over roughened surfaces. Comprehensive summaries of the fundamental fluid dynamics studies with significant wall roughness were presented by Zhang, Lee and Ligrani [3] and Bons et al.[4] Boundary layer thickening and increased turbulent diffusion in the wakes generated by rough surfaces were common observations. In high free stream turbulence environment, the diffusion from the wake to surrounding free stream flow became important, [3]. Roberts

1 Graduate Res. Assist., currently at Elliot Turbines Inc. , PA
2 Graduate Res. Assist.
3 Visiting Professor
4 Professor of Aerospace Engineering, corresponding author cxc11@psu.edu

and Yaras [5] investigated boundary layer transition under the influence of surface roughness and free stream turbulence. They found a strong coupling between the location of transition inception in separation bubbles and the level of mean roughness height. McIlroy et al. [6] recently introduced a new approach for scaling of actual turbine blade roughness on an experimental model of a rough turbine blade. A scaling factor was determined by matching the non-dimensional roughness of a typical airfoil at a certain engine operating condition. Bons and McClain [7] reported the effect of real turbine roughness with pressure gradient on heat transfer. Rough surface effects on un-cooled turbine blades and film cooled turbine vanes were studied by Bogard et al. [8,9]. A significant degradation in adiabatic cooling effectiveness was measured. They also noted that the degradation is much greater on an airfoil suction side cooling configuration when compared to a flat plate cooling configuration. The rough surface influence on TBC applied gas turbine hot section components was investigated by Bunker [10]. The changing heat transfer character of the TBC surfaces with polishing was demonstrated. They also showed that the flow-path steps produced elevated levels of heat transfer on smooth surfaces. However, artificially roughened surfaces did not experience additional heat transfer enhancements due to increased TBC roughness levels. Yun et al. [11] investigated the performance degradation due to blade surface roughness in a single stage axial flow turbine. Typical roughness levels due to in-service surface degradation were simulated. They reported severe degradation of turbine efficiency when the stator and rotor blades were artificially roughened simultaneously. They observed that the roughening of the stator suction side was more damaging in terms of the turbine performance than that of the stator pressure side roughening. A roughened stator alone produced higher stage losses than a roughened rotor. Boyle and Senyitko [12] measured total pressure loss in a linear cascade for a wide range of Reynolds numbers and proposed a roughness transition model from their experiments. Boynton et al. [13] showed that a reduction in blade surface roughness from 10 μm (rough) to 0.8 μm (polished) increased turbine efficiency by 2.1 % in a two-stage high-pressure fuel turbo-pump.

The current study aims to use the physical flow modifying character of artificial wall roughness in reducing the tip leakage mass flow rate in an axial turbine rotor. The aerodynamic character of tip leakage flows were investigated by a large number of investigators in linear cascades and rotating turbine facilities in the past. A comprehensive literature review of tip leakage flows in turbines with smooth casing is included in the references [15,16,17,18,19 and 21].

Although most of the past roughness related studies relied on carefully documented roughness data from sample turbine blades removed from actual service, the current effort uses relatively larger mean roughness heights (66 μm and 141 μm). In this study, larger mean surface roughness heights were used in an effort to beneficially influence the development of a tip vortex for stage efficiency improvements. The typical mean roughness height range used by most previous studies dealing with the understanding of turbine performance degradation and heat transfer augmentation was ranging from 3.5 μm (typical smooth wall) to 57 μm (erosion + deposits), as presented by [3,4]. The pitted or spalled hot section components were characterized with an approximate mean roughness height of 28 μm.

EXPERIMENTAL SETUP & OPERATION

Turbine Research Facility: The facility used for the current research, shown in Figure 1 is the Axial Flow Turbine Research Facility (AFTRF), at The Pennsylvania State University.

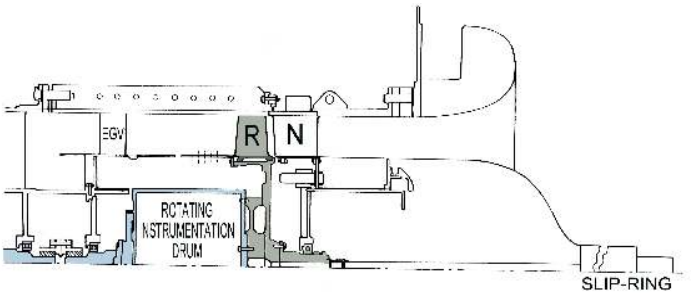

Figure 1 Axial Flow Turbine Research Facility (AFTRF), a cold flow HP turbine stage

A detailed description of the characteristics of this rig is available in Lakshminarayana et al [14], and Camci [15]. The turbine is a large-scale, low speed, cold turbine stage with many characteristics of modern high-pressure turbine stages. The total pressure and total temperature ratios across the stage are small and air flow through the facility is generated by a four

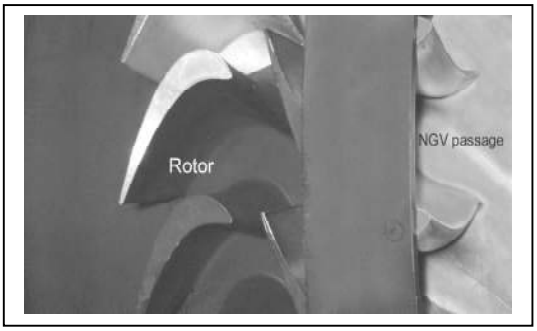

Figure 2 29 bladed rotor and the NGV assembly

stage axial fan located downstream of the turbine. The rotor hub extends 1.7 blade tip axial chord length beyond the rotor exit plane, as marked "Rotating Hub'" in Figure 1. Some of the important design performance data is listed in Table 1, while Table 2 lists important blade design parameters, including reaction at blade hub and tip sections. Axial radial and tangential components of the rotor inlet flow measured just downstream of the NGV assembly is shown in Figure 3. A comparison of the measured rotor inlet conditions with the design data is also given in Figure 3.

Inlet Total Temperature;T_{o1} (K)	289
Inlet Total Pressure;P_{o1} (kPa)	101.36
Mass Flow Rate;Q (kg/sec)	11.05
Rotational Speed; N (rpm)	1300
Total Pressure Ratio; P_{o1}/P_{o3}	1.0778
Total Temperature Ratio; T_{o3}/T_{o1}	0.981
Pressure Drop; P_{o1}-P_{o3} (mm Hg)	56.04
Power; P (kW)	60.6

Table 1 AFTRF Facility Design Performance Data

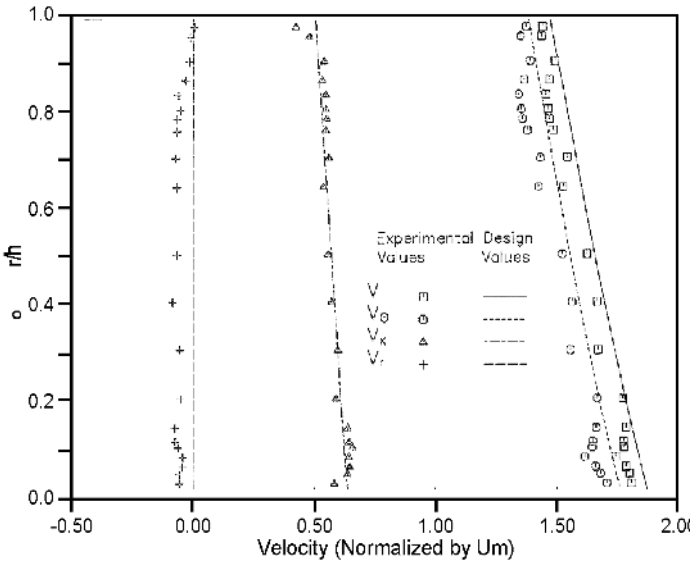

Figure 3 Rotor inlet flow conditions in (AFTRF) measured and design values

Instrumentation: Instruments used for monitoring the performance parameters consist of thermocouples, pitot-static probes and total pressure probes. Phase-locked stage exit total pressures are measured using a fast Kulite dynamic pressure transducer XCS-062-5D. The transducer element has a natural frequency of 150 kHz. The sensor is mounted with a B-screen and is known to have a flat magnitude and phase response up to 20 kHz. The sensor is a sealed cylindrical tube of diameter 1.575 mm, rated at 5 psid, and operates in a differential mode. The Kulite transducer is flush mounted into a square cut cylindrical probe tip of diameter 3.175 mm. The ratio of probe dip diameter to blade spacing (102.8 mm) is 1/32.4. The square cut face gives the probe an acceptance angle of ±10 degrees. The details of the influence of flow incidence on the total pressure measurements from the Kulite probe is presented in Appendix-A.

The probe is located 0.3 chords downstream of the rotor exit plane and is oriented to the absolute velocity vector at the tip (25.4 degrees CCW from axial). The probe is mounted in a computer/stepper motor controlled radial traverse system. AFTRF operational characteristics, data acquisition/processing details and other instrumentation characteristics can be found in Dey, Rao and Camci [16,17,18].

Data Acquisition: Data acquisition system is controlled by a virtual instrument (VI) setup using LabView. The speed is measured using the 6000 pulses per revolution signal generated by the shaft encoder. Data is acquired and averaged over a minute. The traverse mechanism and high speed data acquisition is controlled by a personal computer and a National Instruments PCI-6110E interface. This board is capable of simultaneously sampling its four channels at a maximum rate of 1.25 Ms/sec. The data acquisition is initiated by a trigger pulse (once per revolution) and is subsequently controlled by a clock pulse that has 6000 pulses per revolution. A BEI optical shaft encoder, Model H25 is mounted on the turbine shaft. The data acquisition is thus phase-locked and is conducted at a frequency of 132 kHz (6000 points per revolution). Frequency spectra at various locations show three peaks, at the blade frequency of 132 kHz (6000 points per revolution). Frequency spectra at various locations show three peaks, at the blade passing frequency and its harmonics. Additionally, the energy contained in the signal at frequencies above 12 kHz is 20 dB less than that at the 2 BPF and 30 dB less than that at the BPF. Hence, the signal was low-pass filtered at 20 kHz. At each radial location 200 ensembles of the rotor exit absolute total pressure are acquired and averaged. The probe is radially moved in steps of 1/16 inch.

Rotor hub-tip ratio	0.7269
Blade Tip Radius; R_{tip} (m)	0.4582
Blade Height; h (m)	0.1229
Relative Mach Number	0.24
Number of Blades	29
Axial Tip Chord; (m)	0.085
Spacing; (m)	0.1028
Turning Angle; Tip / Hub	95.42^o / 125.69^o
Nominal Tip Clearance; (mm)	0.9
Reaction, Hub / Tip	0.197 / 0.519
Reynolds Number ($\div 10^5$) inlet / exit	(2.5~4.5) / (5~7)

Table 2 AFTRF Stage Blade & Vane Data

Signal Processing and Uncertainty Estimates: The results are presented in the form of an instantaneous total pressure coefficient, as defined by Equation (1). Radial distributions of the total pressure coefficient are computed as shown in Equation (2) for passage averaged values and Equation (3) for rotor averaged values.

$$C_{pt}(i,j) = \frac{\overline{P}_{03}(i,j) - P_{01}}{\frac{1}{2}\rho U_m^2} \qquad (1)$$

$$C_{pt,av}(j) = \sum_{i}^{i+206} C_{pt}(i,j) \qquad (2)$$

$$\overline{C}_{pt}(j) = \sum_{i=1}^{6000} C_{pt}(i,j) \qquad (3)$$

The propagation of uncertainty, calculated as per Kline and McClintock [19], results in an uncertainty of 0.58% of the nominal total pressure coefficient with a 95 % confidence level. The details of the uncertainty analysis is given in Appendix-A.

Tip Clearance: The turbine rotor tip clearance distribution is shown in Figure 4. Five of the 29 rotor blades have a relatively larger tip gap height (blade # 17,18,19,20,21). The average gap height of these blades is 1.40% blade height, as compared to the nominal gap height of 0.72%. Table 3 also provides the details of rough wall definitions used in this study.The contour plots of the stage exit total pressure coefficient C_{pt} shown in Figures 5,6,7 and 8 contain the tip vortices from blades #19,20,21,22,23 as shown in Figure 4. The measurements shown for original turbine casing OCA (dashed line) in Figure 4 are obtained from the original casing surface without any casing treatment. The smooth plastic layer SPL is 0.318 mm thick including the double-sided tape corresponding to a treatment thickness of 0.26 % blade height. The Fine Sand Paper's (FSP) treatment thickness including the double-sided tape is also 0.318 mm by design. The Coarse Sand Paper CSP is slightly thicker (0.394 mm) than the Fine Sand Paper FSP.

Casing Roughness: The original casing surface was artificially roughened by applying commercial grade sandpaper to the casing with double-sided adhesive tape. Two grades of sandpaper used were a coarse 100 grit paper (mean roughness height k=141 μm) and a fine 220 grit paper (mean roughness height k=66 μm). A smooth, thermoplastic layer was also separately applied in a few experiments to obtain a smooth reference surface. This was done to isolate the effect of artificially roughening the casing surface from the effect of tip gap height reduction due to sand paper thickness. The nominal thickness of the applied fine sand paper was 0.318 mm or 0.26% h. This caused the tip gap height to be reduced and is shown in Figure 4 by the curve FSP. The coarse sand paper was 0.394 mm thick (0.30 %h).The sand paper, double sided tape and smooth thermoplastic reference surface thicknesses were measured using an instrument accurate to ± 0.0002 inch. Individual blade tip clearances were also measured from the AFTRF original casing position with a measurement accuracy of ± 0.001 inch.

RESULTS FROM ROUGH CASING EXPERIMENTS

Baseline results without any casing treatment: The total pressure coefficient contour map without roughness is shown in Figure 5. This figure documents the original operational characteristics of the AFTRF without any casing treatment (OCA). Boundaries at the hub, the mid-span and the casing, are marked in the contour plots. Above the casing boundary line the blade number and the corresponding tip clearance is marked. The contour map contains three blades with large gap heights (#'s 19, 20, and 21) and two subsequent blades with nominal tip gap (t/h=0.83 % and 0.77%). These over-tip-leakage (OTL) vortices (#19,20,21) are characterized by the large footprint, in comparison to that of the neighboring blades (#22 and #23) that have tip clearance values about 0.83 %.

	CASING TREATMENT DEFINITION		t/h % Blade #19	t/h % Blade #20	t/h % Blade #21	t/h % Blade #22	t/h % Blade #23
OCA	ORIGINAL TURBINE CASING	▲	1.54	1.39	1.40	0.83	0.77
SPL	SMOOTH PLASTIC LAYER	■	1.28	1.13	1.14	0.57	0.51
FSP	FINE SAND PAPER k=66 μm	■	1.28	1.13	1.14	0.57	0.51
CSP	COARSE SAND PAPER k=141μm	◆	1.24	1.09	1.10	0.53	0.47

Table 3 Casing treatment definition

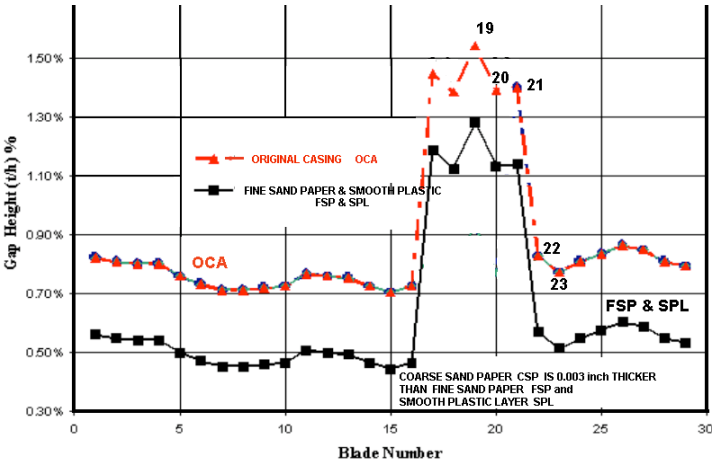

Figure 4 Tip clearances for 29 rotor blades with and without casing roughness in (AFTRF)

These large vortices influence the top 25% of the passage flow and a significant part of the space between adjacent blades. The OTL vortices are also bounded by curves that denote the size and position of the vortices when the gap height of these blades was at the nominal level (0.72%). Clearly the increased gap heights have caused the OTL flow structures from blades #19 and #20 to move towards blade suction side. For the blade sector shown, the largest total pressure defect is seen for blade #19, which has the largest tip gap.

Smooth Casing Surface: The total pressure coefficient distribution in the measurement plane using a smooth plastic layer (SPL) at a uniformly reduced tip gap height is shown in

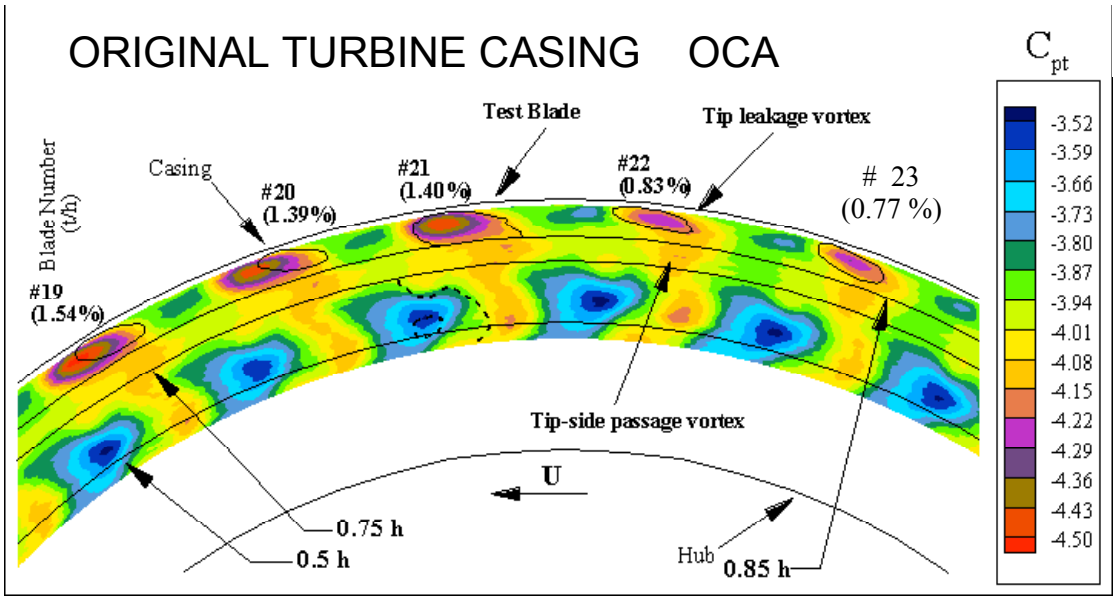

Figure 5 C_{pt} distribution at 30 % downstream of AFTRF rotor, **ORIGINAL TURBINE CASING** OCA

Figure 6. The treatment thickness of the SPL is 0.26% of blade height including the double sided tape.. The tip gap height of each blade is noted above the casing boundary. The tip gap height reduction leads to the expected reduction in total pressure defect for all blades, as compared to the total pressure coefficient observed in Figure 5. The smallest tip gap height obtained is t/h = 0.51% for blade #23 and consequently the corresponding tip leakage vortex is very weak and contained within the wake. The expected movement of the tip leakage vortices to the right is also observed. The green zones between the subsequent tip leakage vortices have relatively higher total pressure.

Fine Casing Roughness (220 Grit, k=66 μm): The total pressure coefficient distribution shown in Figure 7 was obtained after applying 220 Grit commercial grade sandpaper to the casing inner surface. The thickness of the applied treatment is 0.26% blade height. It is clear that the artificially introduced surface roughness has considerable effect on both the leakage flow and the tip-side passage vortex. The OTL vortices of blades #19,20 and 21 shown are greatly reduced in size. Their individual total pressure defect is also substantially reduced. The tip leakage vortex is contained (or merged) within the wake and is located to the right of the tip-side passage

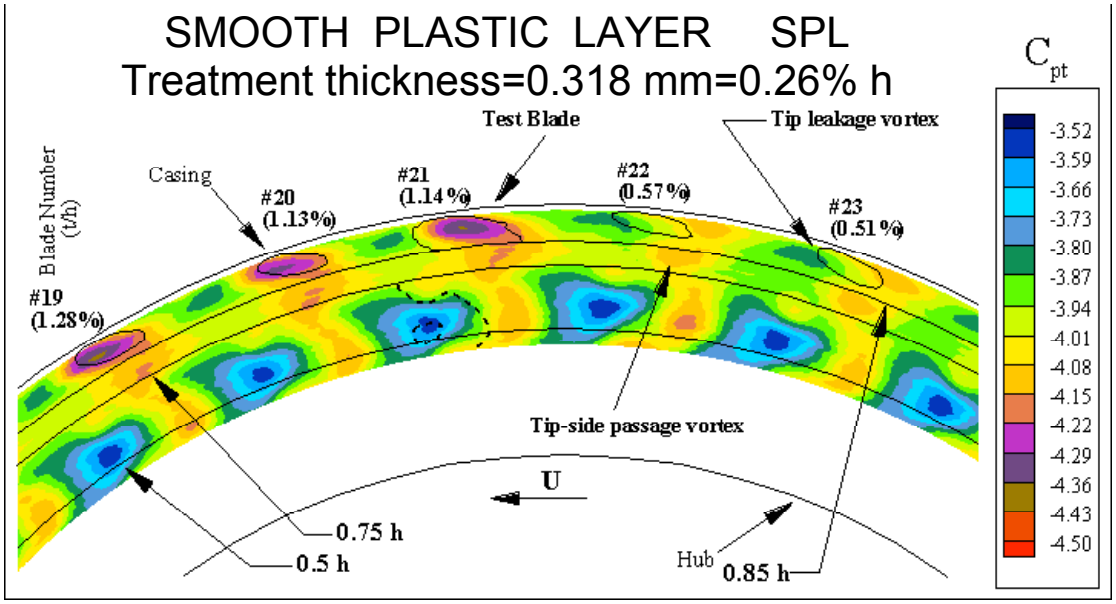

Figure 6 C_{pt} distribution at 30 % downstream of AFTRF rotor, **SMOOTH PLASTIC LAYER** SPL

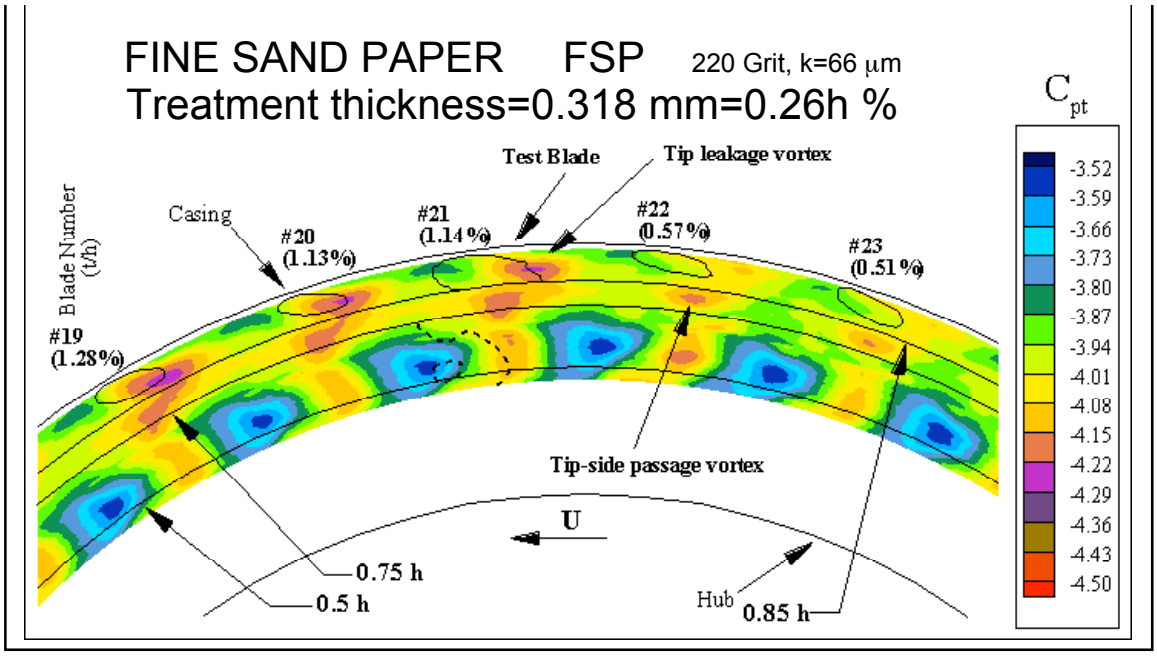

Figure 7 C_{pt} distribution at 30 % downstream of AFTRF rotor, **FINE SAND PAPER** FSP 220 Grit, k=66 μm

vortex. The passage vortices now are more visible because the tip vortex system is weakened by the implementation of casing roughness. The relatively strong tip vortices previously shown for the baseline case without any treatment in Figure 5 were clearly influencing the passage vortex. This influence is mainly due to a strong turbulent shear applied in the opposite direction to the passage vortex by the tip vortex.. The tip leakage vortices of blades #22 and #23 are significantly weakened and completely mixed in with the wake fluid at allocation over the passage vortices that are clearly visible. Non of the red-brown C_{pt} areas with strong total pressure defect are visible after the casing treatment with fine sand paper. The increased casing surface roughness is expected to locally increase turbulent kinetic energy within the tip gap, leading to greater total pressure loss. Thus the secondary kinetic energy associated with the OTL vortex in the blade passage is reduced and the over tip leakage fluid is relatively weakened. The application of fine sand paper to the casing area corresponding to the rotor blade may also influence the development of the near casing flow between the subsequent blade tips. The character of three-dimensional casing boundary layers and the leakage flow entrance conditions to the tip gap area are altered.

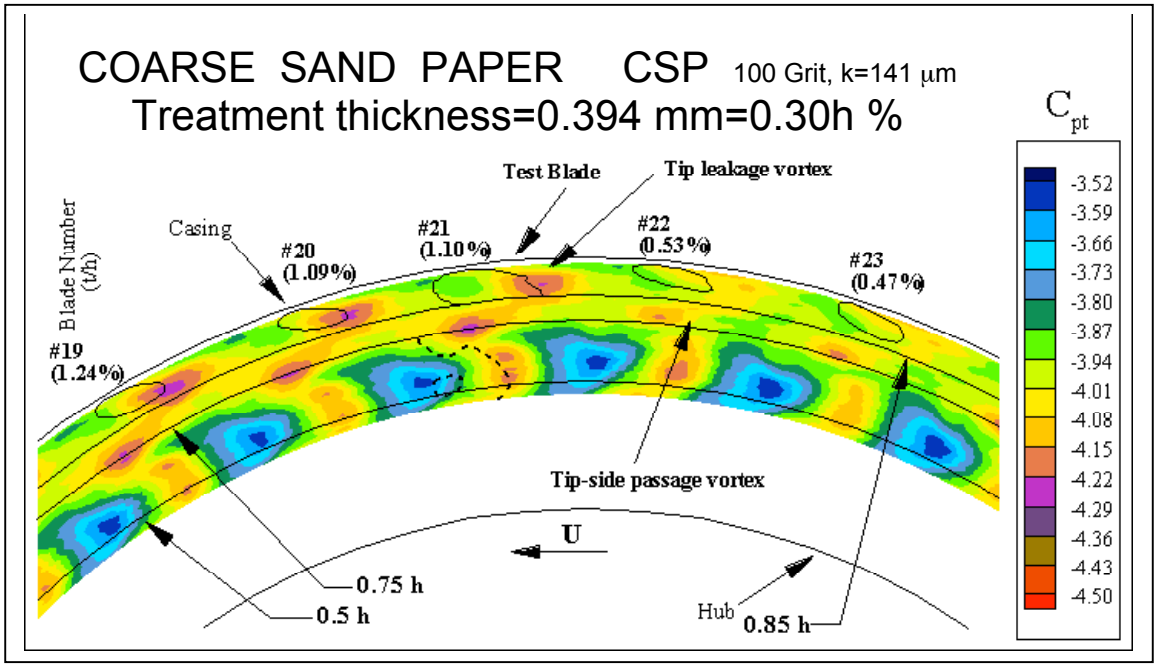

Figure 8 C_{pt} distribution at 30 % downstream of AFTRF rotor, **COARSE SAND PAPER** CSP 100 Grit, k=141 μm

The tip-side passage vortices appear to be stronger and especially so at the larger tip gap heights. This is partly due to the reduced interaction between the tip leakage flow and the tip-side passage secondary flow. The passage flow cores with high momentum (dark blue) are shifted considerably to the left and this is probably due to the reduced blockage from the tip vortex and the new position of the tip-side passage.

Coarse Casing Roughness (100 Grit, k=141 μm): Figure 8 is a contour plot of the total pressure field downstream of the rotor with coarse sand paper applied on to the casing. While the treatment thickness (0.3% h) is slightly greater than the previous two treatments, the difference of 0.04% h is believed to be too small to have a strong effect on the tip gap flow. Hence, any differences seen may be attributed to the increased surface roughness. The effect of coarse roughness on the tip leakage flow appears to be similar to that of fine sandpaper. The tip leakage vortices are greatly reduced in area and the total pressure field within the vortices has much less defect when compared to smooth wall. The weakened tip leakage vortices at the small gap heights are again mixed in with the blade wakes. The tip-side passage flow also appears to be more uniform across the passage. The tip-side passage vortices are visible due to the reduced shear interaction with the tip leakage flow. The reduced interaction between the secondary flows near the blade tip is a result of reduction in leakage flow momentum exiting the tip gap. The movement of the passage core to the left is also observed and hence it can be concluded that this is due to the increased surface roughness. Figure 8 shows a strong beneficial influence of using an artificially roughened casing surface using sandpaper type wall roughness. The weakened tip vortex system and a reduced shear interaction of the tip vortex and the passage vortex system is clearly observed.

Passage to passage Cp variation near the casing Since the C_{pt} measurements are phase-locked, a comparison of the total pressure (wake) profile for different casing roughness treatments in different passages is illuminating. The wake profiles in Figure 9 for r=0.96h show that the artificially roughened casing leads to considerable reduction in wake defect, in the range of 0.3 q_m to 0.4 q_m. The wake depth of the blade # 21 is reduced by 0.38 q_m, which is greater than the 0.14 q_m reduction obtained by the effect of reducing the gap height only. Thus, the effect of artificially roughening the casing inner surface is about 1.7 times the effect of reducing the tip gap height. The total pressure defect reduction is also greater at the larger tip gap heights. For the wake profiles shown in Figure 9, there is small difference between the smooth wall and fine roughness wake deficits at the smaller tip gap heights. There is however a global shift in the wake profiles to the right. The effect on the passage core is also observed in the wake profiles at mid-span (0.57h), shown in Figure 10. The wake profile may be observed to have slightly shifted to the left, a behavior also seen in the contour plot. The wake depth however remains almost the same for all casing treatments.

The wake profiles at r = 0.96 h, due to the increased surface roughness are quite similar to those obtained with the fine surface roughness as shown in Figure 9. This observation implies that the flow influence of surface roughness is not enhanced significantly by increasing the average roughness height from k=66 μm to 141 μm. The wake profiles close to mid-span, shown in Figure 10 also indicate that the effect of surface roughness is unchanged by the increase in the roughness quality of the casing inner surface.

Comparison of the Averaged Total Pressure Coefficient: The circumferentially averaged total pressure coefficient, computed for the passage containing the tip leakage vortex of blade #21 (t/h=1.40%, without casing treatment) with different casing roughness treatments is shown in Figure 11. The red baseline with solid square symbol is the average of five reference blades that are # 17,18,19,20 and 21. The decrease in tip gap height by 0.26%h without artificial roughness (smooth plastic layer SPL) reduces the total pressure defect observed in the region from 0.85h to 1.0h. The introduction of surface roughness doubles the total pressure defect reduction over the entire passage, from $0.05q_m$ to $0.1q_m$ at the location 0.93h. The beneficial effect obtained from the two roughness levels studied (100 grit and 220 grit) are comparable with a previous tip de-sensitization study using tip injection described in Rao and Camci [17,18].

CONCLUSIONS

The present paper aims to understand the performance benefits of implementing artificial casing roughness in axial flow turbines.

Although there have been many recent studies in understanding the influence of roughness on aerodynamic flows in turbomachinery systems, our knowledge on the influence of artificially introduced wall roughness applied on the inner part of the casing is very limited.

Phase-locked measurements of the absolute total pressure were conducted at the turbine stage exit using a high-frequency-response total pressure probe.

A partial segment of the turbine casing was artificially roughened by using a roughness layer of two different mean roughness heights.

A smooth wall as a baseline case was also investigated by attaching a smooth layer of equivalent thickness to the casing surface. Artificially roughening the casing surface significantly reduced the leakage mass flow rate and the momentum deficit in the core of the tip vortex.

An artificially roughened casing in relative motion clearly reduces momentum deficit that is in the core of each tip vortex. The measurements also show that the significant shearing between the tip vortex and the passage vortex is weakened in the last 15 % of the blade height.

The existence of a rough wall measurably reduces the tip leakage mass flow rate. The character of three-dimensional casing boundary layers and the leakage flow entrance conditions to the tip gap area are altered.

The tip-side passage vortices appear to be stronger and especially so at the larger tip gap heights. This is partly due to the reduced interaction between the tip leakage flow and the tip-side passage secondary flow.

The passage flow cores with high momentum (dark blue) are shifted considerably to the left (in a direction from the suction side to the pressure side)and this is probably due to the reduced blockage from the tip vortex and the new position of the tip-side passage vortex.

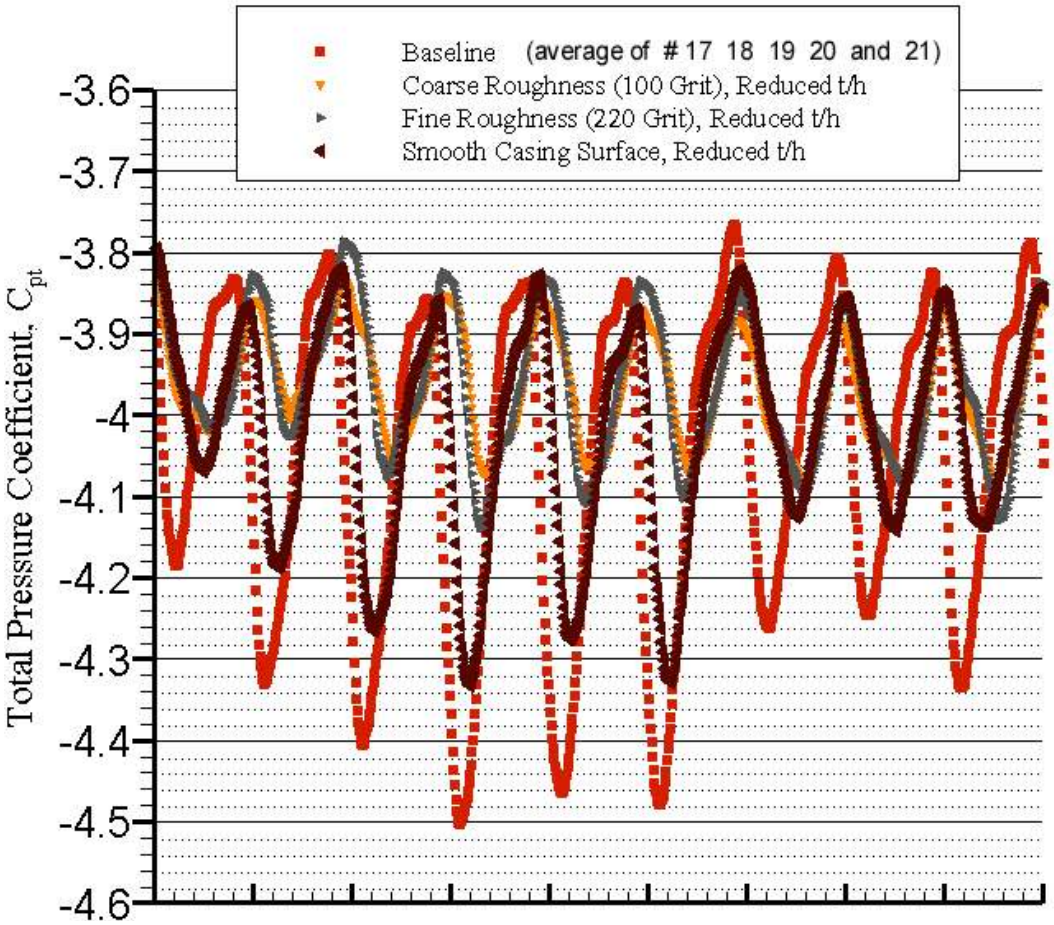

Figure 9 C_{pt} distribution near tip ($r = 0.96\ h$) with significant casing treatment influence

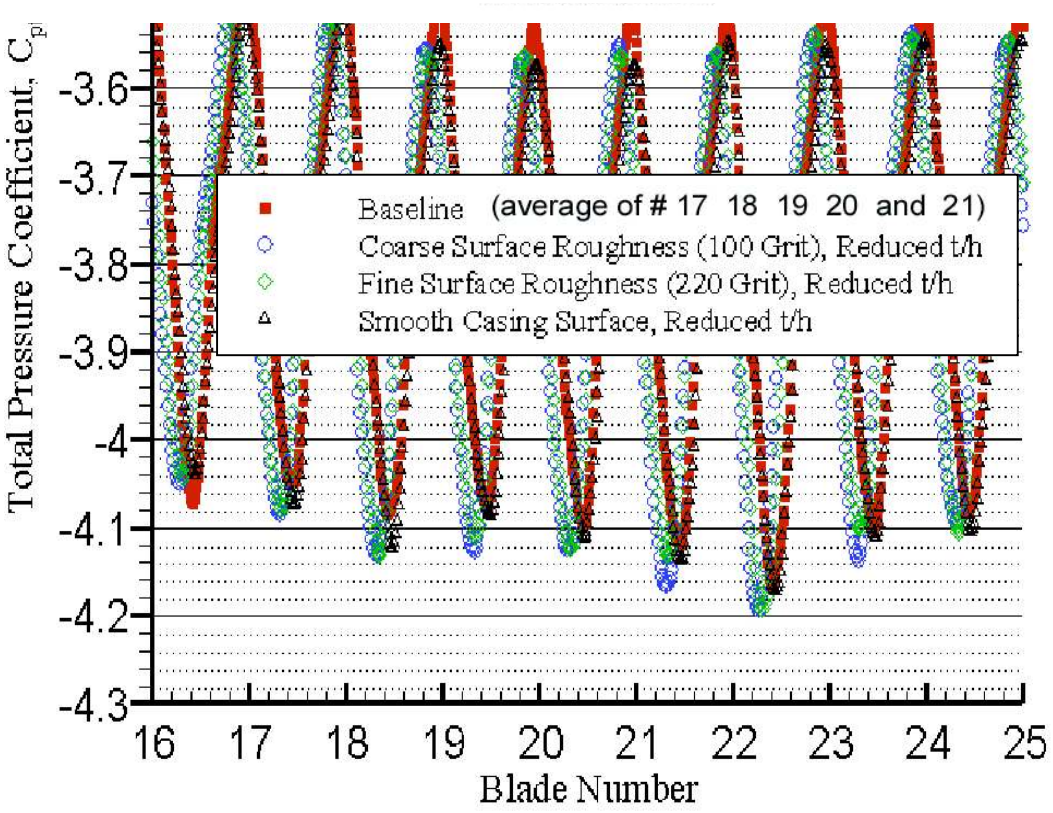

Figure 10 C_{pt} distribution at mid-span (r=0.57h) with minimal casing treatment influence

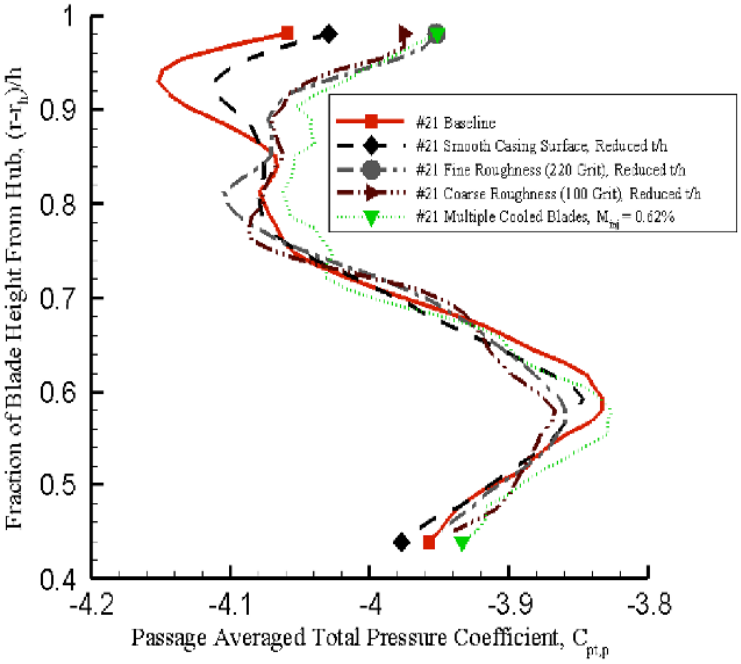

Figure 11 Circumferentially averaged total pressure distribution along the radius

APPENDIX - A

The sensitivity of the total pressure coefficient to probe incidence was tested at two radial locations in the AFTRF. Measurement sensitivity to exit flow angle was measured by rotating the probe in increments of 5°, on either side of exit flow direction (stationary frame) α_3 = 25.4° measured from axial direction.. This was done at two radial locations, 0.93h (near tip region) and 0.49h (mid span). Counterclockwise (CCW) rotation of the probe is positive and makes the probe more tangential with every increment. The rotor averaged, and passage averaged total pressure coefficient for blade #21, are shown in Figure 12. The absolute velocity vector at mid span is at an angle of 29.19° from axial, corresponding to an incidence angle of 3.79°. The mean value of $C_{pt,P}$ at mid-span in a ±15° range is -3.916 and all values in this range lie within the uncertainty band of δC_{pt} = ± 0.024. Furthermore, the passage averaged coefficient for blade #21 indicates that the blade passage behaves almost identically as the rest of the rotor. At 0.93h however, the difference between the rotor averaged and passage averaged values is considerable, due to the large leakage vortex. Passage averaged coefficient in the range -25° to 10° are within uncertainty limits of the mean value ($C_{pt,P}$ = -4.22), computed for the range ±15°. The value at 15° is just outside the uncertainty band. McCarter, et al. [21] measured lower relative tangential velocity in the region dominated by the leakage vortex. This means that the leakage vortex approaches the probe at a negative incidence. Thus, from measurements in the range of -25° to 0° it is possible to conclude that error in the measurement of total pressure associated with the tip leakage vortex of the test blade is within uncertainty bounds

The propagation of C_{pt} uncertainty is calculated by the method derived by Kline and McClintock [20]. The uncertainty in the total pressure coefficient is obtained from Equation **A-2**, which is obtained by differentiating Equation **A-1**,

$$C_{pt}(i,j) = \frac{\Delta P_0}{\frac{1}{2}\rho U_m^2} \quad \text{where} \quad \Delta P_0 = \overline{P}_{03}(i,j) - P_{01} \qquad \text{A-1}$$

$$\frac{\delta_{C_{pt}}}{C_{pt}} = \sqrt{\left(\frac{\delta_{\Delta P_0}}{\Delta P_0}\right)^2 + \left(\frac{\delta_\rho}{\rho}\right)^2 + \left(\frac{2\delta_{U_m}}{U_m}\right)^2} \qquad \text{A-2}$$

where δ is the uncertainty associated with the parameter in the square brackets. The individual uncertainty and nominal value of each measured parameter (used in the denominator) is shown in Table A-1. These in turn are obtained from manufacturer specifications of the precision associated with the measurement.

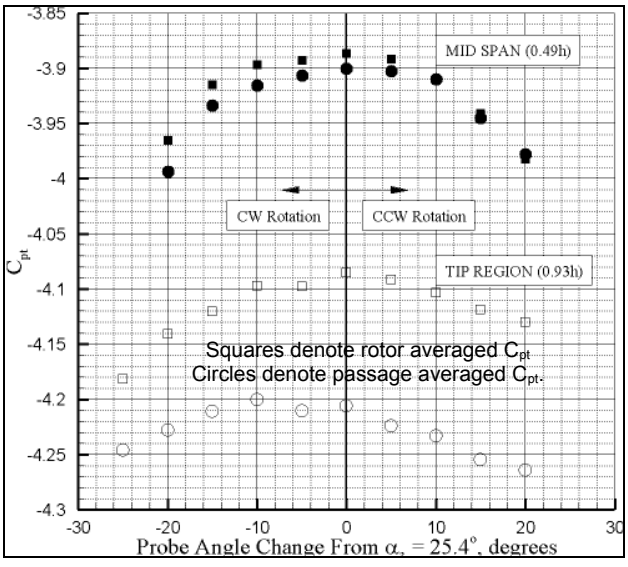

Figure 12 Kulite Probe Response to Incidence angle.

Table A-1: Uncertainty and Nominal Values in Measured Parameters

Parameter	Precision Error	Uncertainty	Nominal Value
ΔP_0	0.1% of $34.474*10^3$ (kPa)	±34.474 (Pa)	7471.387 (Pa)
T_{amb}	±0.5 (K)	±0.5 (K)	300 (K)
P_{amb}	0.1%	±100 (Pa)	98700 (Pa)
N	±1 (rpm)	±1 (rpm)	1328 (rpm)

ACKNOWLEDGMENTS

The authors are indebted to Mr.Harry Houtz, Mark Catalano, and Kirk Hellen for their outstanding technical support. The authors acknowledge the valuable support from the Department of Aerospace Engineeering at Penn State University.

Table A-2: Uncertainty in Derived Parameters

Parameter	Uncertainty
$\frac{\delta_{C_{pt}}}{C_{pt}}$	±0.0058
$\frac{\delta_{\Delta P_0}}{\Delta P_0}$	±0.00461
$\frac{\delta_{\rho}}{\rho}$	±0.0035
$\frac{\delta_{U_m}}{U_m}$	$\pm 7.53*10^{-4}$

NOMENCLATURE

C_{pt}	Total pressure coefficient, see equation (1)
C_{ax}	Rotor tip axial chord length
CSP	Coarse sand paper
FSP	Fine sand paper
i	Circumferential position indicator
j	Radial position indicator
h	Rotor blade height
k	Average roughness height
OCA	Original turbine casing (untreated)
p_{o1}, P_{o1}	Stage inlet total pressure, Pa
p_{o3}, P_{o3}	Stage exit total pressure, Pa
r	Radius
SPL	Smooth plastic layer
t	Gap height between blade tip and outer casing, m
t_r	Distance of reattachment line from pressure-side corner, m
U_m	Rotor blade speed at mid-height location
V	Velocity
θ,x,r	Tangential, axial, radial components

REFERENCES

1. Nikuradse, J., 1933, "Laws of Flow in Rough Pipes," NACA TM 1292, National Advisory Committee on Aeronautics.
2. Schlichting, H., 1936,"Experimental Investigation of the problem of Surface Roughness," NACA TM-832, National Advisory Committee on Aeronautics.
3. Zhang, Q.,Lee, S.W., Ligrani, P.M., 2004,"Effects of Surface Roughness and Turbulence Intensity on the Aerodynamic Losses Produced by the Suction Surface of a Simulated Turbine Airfoil,".
4. Bons, J.P., Taylor, R.P., McClain, S.T. and Rivir, R.B., 2001, "The Many Faces of Turbine Surface Roughness," ASME Trans. Journal of Turbomachinery, Vol.123, pp.739-748.
5. Roberts, S.K. and Yaras, M.I., 2005, "Boundary Layer Transition Affected by Surface Roughness and Free Stream Turbulence," ASME Trans., Journal of Fluids Engineering," Vol.127, pp.449-457.
6. McIlroy, H.M., Budwig, R.S. and McEligot, D.M., 2003, "Scaling of Turbine Blade Roughness for Model Studies," Proceedings of the ASME IMECE, IMECE 2003-42167, Washington, D.C.
7. Bons, J.P., McClain, S.T., 2004, "The Effect of Real Turbine Roughness with Pressure Gradient on Heat Transfer," ASME Trans. Journal of Turbomachinery, Vol.126, pp.385-394
8. Bogard, D.G., Schmidt, D.L., Tabbita, M., 1998,"Characterization and Laboratory Simulation of Turbine Airfoil Surface Roughness and Associated heat Transfer," ASME Trans. Journal of Turbomachinery, Vol.120, pp.337-342.
9. Bogard,D.G., Snook D., Kohli, A., 2003, "Rough Surface Effects on Film Cooling on the Suction Side Surface of a Turbine Vane," Proceedings of the ASME IMECE, IMECE 2003-42061, Washington, D.C.
10. Bunker, S.R., "The Effect of Thermal Barrier Coating Roughness Magnitude on Heat Transfer with and without Flowpath Surface Steps," Proceedings of the

ASME IMECE, IMECE 2003-41073, Washington, D.C.
11. Yun, Y.I., Park, I.Y., Song, S.J., 2004, "Performance Degradation Due to Blade Surface Roughness in a Single-Stage Axial Turbine," ASME paper GT 2004-53094.
12. Boyle, R.J. and Senyitko,R.G., 2003, "Measurements and Predictions of of Surface Roughness Effects on Turbine Vane Aerodynamics," ASME paper GT 2003-38580.
13. Boynton, J.L. Tabibzadeh, R., and Hudson, S.T., 1993, "Investigation of Rotor Blade Roughness Effects on Turbine Performance," ASME Trans. Journal of Turbomachinery, Vol.115, pp.614-620.
14. Lakshminarayana, B., Camci, C., Halliwell, I., and Zaccaria, M., 1996, "Design and Development of a Turbine Research Facility to Study Rotor-Stator Interaction Effects," International Journal of Turbo and Jet Engines, 13, pp.155-172.
15. Camci, C., 2004, Experimental and Computational Methodology for Turbine Tip De-sensitization. *VKI Lecture Series 2004-02*, "Turbine Blade Tip Design and Tip Clearance Treatment," 2004.
16. Dey, D., 2001, "Aerodynamic Tip Desensitization in Axial Flow Turbines," Doctoral Thesis, Pennsylvania State University, December 2001.
17. Rao, N. and Camci, C., 2004, "Axial Turbine Tip Desensitization by Injection from A Tip Platform Trench. Part1: Effect Of Injection Mass Flow Rate," ASME paper 2004-53256.
18. Rao, N. M., and Camci, C., 2004, "Axial Turbine Tip Desensitization by Injection from a Tip Platform Trench. Part 2- Leakage Flow Sensitivity to Injection Location," *ASME* Paper No. GT2004-53258.
19. Rao, N. M., and Camci, C., 2004, "A Flow Visualization Study of Axial Turbine Tip Desensitization by Coolant Injection from a Tip Trench," *ASME* Paper No. IMECE2004-60943.
20. Kline, S.J., McClintock, F.A., 1953, "Describing Uncertainties in Single-Sample Experiments." Mechanical Engineering, Vol.75, pp.3-17.
21. McCarter, A., "Investigation of Tip Clearance Flow Fields in a Turbine Rotor Passage," Masters Thesis, Pennsylvania State University, May 2000.